Lowland Technology International date; Volume 22(2): 280-289
International Association of Lowland Technology (IALT): ISSN 1344-9656

Research Paper

Shear strength characteristic of unsaturated undisturbed black volcanic ash soil in Kumamoto under static and cyclic loading

O. A. Putra [1], N. Yasufuku [2], A. Alowaisy [3], R. Ishikura [4], A. Rifa'i [5], and Y. Kawaguchi [6]

ARTICLE INFORMATION

Article history:

Received: 03 February, 2020
Received in revised form: 20 June, 2020
Accepted: 27 June, 2020
Publish on: 06 September , 2020

Keywords:

Black volcanic ash
Direct shear box
Shear strength
Cyclic
Pore size distribution

ABSTRACT

Black volcanic ash soil which is also known as Kuro-boku soil in Japan is a problematic type of soil. Kuro-boku is usually rich with allophane minerals, which are characterized by unique problematic properties. Through this paper, the shear strength and characteristics of the black volcanic ash soil collected at Kumamoto slope failure after earthquake 2016 were studied using three main approaches. The chemical composition of the black volcanic ash soil was investigated using the X-ray fluorescence analysis. Furthermore, the soil structure disturbance effect due to the earthquake shakes on the total shear strength was evaluated using a simple method that considers the pore size distribution that is reflected from the soil-water characteristic curve. In addition, the constant volume direct shear box considering static and cyclic tests were carried out. It was found that the main chemical content of the black volcanic ash soil is allophane which accounts for about 94%. Furthermore, the undisturbed samples exhibit a unimodal pore structure, and the disturbed showed a bimodal pore. Since the pore structure of the disturbed sample is unstable, the static shear strength tends to be lower and the degradation index value is higher than that of the undisturbed sample.

1. Introduction

Black volcanic ash soil which is also known as Kuro-boku soil in Japan is a problematic type of soil (Kitazono et al., 1987; Mshana et al., 1993). Kuro-boku (organic cohesive volcanic ash soil) is usually rich with the allophane minerals, which are characterized by unique problematic properties. As reported by several researchers, black volcanic ash soil has high natural moisture contents varying between 65-160% (Kodani et al., 1975; Japan soil inventory, 2016).

The black volcanic ash soil is typically located in the top layer of natural slopes above the groundwater table with degrees of saturation less than 100 % which can be classified as an unsaturated state. In general soils under unsaturated conditions have higher strength and shear

[1] Graduate student, Geotechnical Engineering Laboratory, Department of Civil Engineering, Faculty of Engineering, Kyushu University, 744 Motooka, Nishi-ku, Fukuoka 819-0395, JAPAN, okriasfino27@gmail.com (Corresponding author)
[2] Professor, Geotechnical Engineering Laboratory, Department of Civil Engineering, Faculty of Engineering, Kyushu University, 744 Motooka, Nishi-ku, Fukuoka 819-0395, JAPAN, yasufuku@civil.kyushu-u.ac.jp
[3] Research Assistant Professor, Geotechnical Engineering Laboratory, Department of Civil Engineering, Faculty of Engineering, Kyushu University, 744 Motooka, Nishi-ku, Fukuoka 819-0395, JAPAN, adel_owaisi@yahoo.com
[4] Associate Professor, Geotechnical Engineering Laboratory, Department of Civil Engineering, Faculty of Engineering, Kyushu University, 744 Motooka, Nishi-ku, Fukuoka 819-0395, JAPAN, ishikura@civil.kyushu-u.ac.jp
[5] Associate Professor, Department of Civil and Environmental Engineering, Faculty of Engineering, Universitas Gadjah Mada, Yogyakarta 55281, INDONESIA, ahmad.rifai@ugm.ac.id
[6] West Nippon Expressway Company Limited, 1-6-20 Dojima, Kita-ku, Osaka City, JAPAN, e3softball81@gmail.com
Note: Discussion on this paper is open until March 2021

resistance in comparison to the saturated condition. However, under heavy rainfall events, the pore water pressure increases leading to the loss of shear strength and slope instability. The black volcanic ash soil covers approximately 31% of the total area of Japan, mainly distributed within the volcanic zones (Yamauchi, 1983). In Kyushu Island, the black volcanic ash soil can be found in the Aso mountain area, Kumamoto city.

In April 2016 an earthquake with a magnitude of 7.0 has struck the Kumamoto area and induced several slope failures around Aso mountain area. It was reported that orange-colored pumice deposits and black volcanic ash soil are dominant in the affected area. According to (Miyabuchi, 2016; Mukonoki et al., 2016; Kiyota et al., 2017; Chiaro et al., 2018), the critical factor that has led to those failures is the reduction in the total shear strength of the volcanic ash soil due to the earthquake load. Also, it was reported that the earthquake caused a significant disturbance to the soil microstructure. Therefore, it is believed that the disturbance has led to damaging the soil microstructure which is directly related to the total shear strength of the soil.

Many researchers have studied the shear strength and mechanical characteristics of the volcanic ash soil in Kumamoto area, especially the orange-colored pumice. However, small attention was given to the shear strength and mechanical characteristics of the black volcanic ash soil. In addition, the fact that the black volcanic ash is highly comprised of allophaneous minerals adds to the complexity, where most of the existing studies focus on the hydrological characteristics rather than mechanical behavior.

Allbrook, 1985 reported that the cohesion and the friction angle of allophaneous volcanic ash soils are generally less than that of non-allophanic soils. This behavior was related to the absence of face-to-face contact which can be normally found in platy minerals.

Through this paper, three main approaches were adopted to evaluate the shear strength and the mechanical characteristics of the black volcanic ash soil. First, the chemical composition of the black volcanic ash soil was studied using the X-ray fluorescence analysis (XRF) technique. Furthermore, the soil structure disturbance influence due to the earthquake shakes on the total shear strength of the black volcanic ash soil was discussed. In general, most of the existing studies investigate the effect of the soil structure disturbance by comparing the total shear strength characteristics using a series of cyclic triaxial tests. In addition, the microstructure characteristics are commonly studied using the Scanning Electron Microscope (SEM) (Qinghui et al., 2016; Ding et al., 2019). These methods need special equipment and skill that are generally not available in common Geotechnical laboratories. Through this paper, the effect of soil structure disturbance on the shear strength characteristics of black volcanic ash was evaluated using a simple methodology where the disturbance on soil structure was indirectly considered by studying the pore size distribution which was reflected from the Soil-Water Characteristic Curve (SWCC) using disturbed and undisturbed samples. Moreover, the constant volume direct shear box was used, where several series of static and cyclic tests were carried out. Finally, the effect of the precipitation events and the changes in the moisture content were considered by testing and comparing saturated and unsaturated samples.

2. Methodology and materials

2.1 Sampling methodology

The undisturbed sampling methodology and molds used for collecting undisturbed black volcanic ash soil samples are illustrated in **Fig. 1**. Sampling was carried out using 6 cm in diameter and 4 cm in height acrylic cylindrical molds. Before sampling, the inner surface of the acrylic mold and the cutter ring were covered with grease oil to reduce the friction and therefore minimize the disturbance. The acrylic containing mold attached to the cutter ring was driven using a plate equipped with a bubble level to cut into the ground. After that, the sample's upper and lower surfaces were trimmed using a spatula. In order to prevent any water loss due to evaporation, samples were kept in sealed plastic bags.

Table 1. Physical properties of the black volcanic ash

Physical properties		Black volcanic ash
Water content	(%)	111-159
Dry density, ρ_d	(g/cm^3)	0.56-0.58
Bulk density, ρ_t	(g/cm^3)	1.18-1.25
Liquid limit	(%)	154-214
Plastic limit	(%)	112-139
Organic matter	(%)	22.9-28.2
Specific gravity	Gs	2.28-2.34
Coefficient of uniformity	U_c	4.33
D_{50}	mm	0.012
Classification by JGS	Volcanic cohesive soil type II (VH_2)	

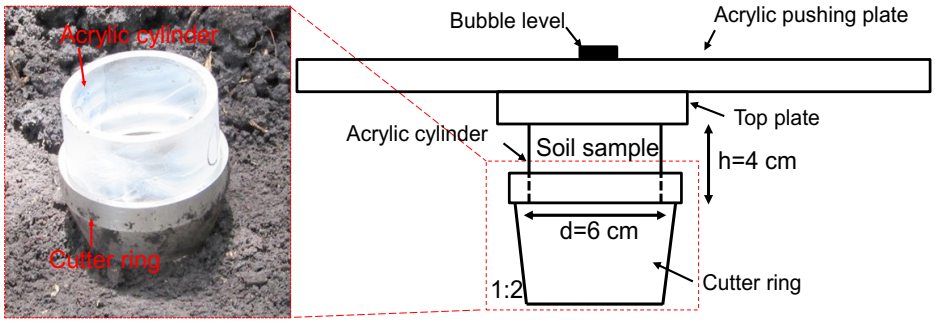

Fig. 1. Sampling setup for undisturbed sample

Fig. 2. Sampling location of the black volcanic ash

2.2 Materials and sampling location

After Kumamoto earthquake 2016, several slope failures occurred around the Aso mountain area. The sampling points were located at the middle and the top boundaries of a large slope failure zone as illustrated in **Fig. 2**. The cross-section of the failure zone at the boundaries mainly comprised of black volcanic ash soil extending approximately to a depth of 1.5 m from the soil surface. Undisturbed and disturbed samples were collected at the slip surface. It must be noted that disturbed samples were prepared with the same natural bulk density and water content as of the undisturbed samples.

The physical properties of the collected black volcanic ash are listed in Table 1. It can be seen that the organic matter content ranges from 22.9 % - 28.2 %. The median grain size D_{50} is approximately 0.012 mm. Consequently, the black volcanic ash soil can be classified as volcanic cohesive soil type II (VH_2) according to the Japanese Geotechnical Society standards (JGS 0051, 2009).

The consolidation test results of the saturated and unsaturated black volcanic ash samples are indicated in **Fig. 3**. It was found that the yield stress corresponding to the unsaturated undisturbed sample is about 105 kN/m^2. Noting that the sampling depth was around 1.5 m, where the soil was subjected to an overburden pressure less than 105 kPa, the collected black volcanic ash in this research can be considered as Over-Consolidated (OC) soil with an Over-Consolidated Ratio (OCR) less than 1. The OCR can be determined using the following equation:

$$OCR = \frac{P_c}{P_o'} \quad [1]$$

where P_c is the yield stress and $P_{o'}$ is the overburden pressure.

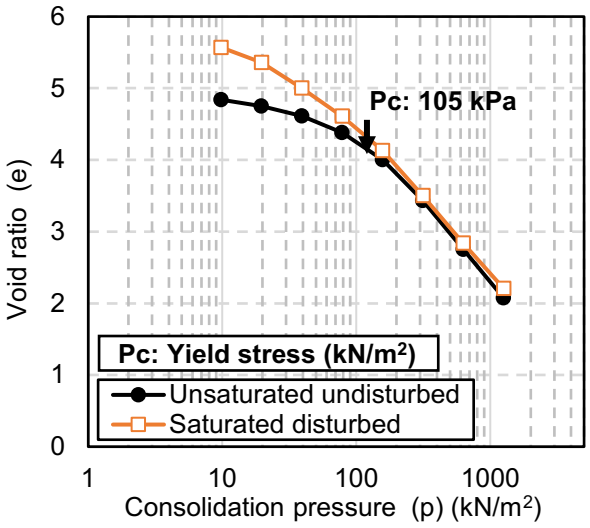

Fig. 3. Consolidation test of the black volcanic ash

2.3 Methodology

2.3.1 X-ray fluorescence analysis (XRF) test

The chemical content of the black volcanic ash was determined using the X-ray diffraction technique (MutiFlex 50kv. 50mA) with an energy dispersive X-ray fluorescence analyzer (Shimadzu EDX-7000 50kv. 1000μA). Only soil particles with diameter less than 2 mm were used to determine the chemical composition of the black volcanic ash soil.

2.3.2 Shearing test

The shear strength characteristics of the black volcanic ash soil were evaluated using the direct shear box (constant volume tests) considering both undisturbed and disturbed samples. In the constant volume tests, the volume of the samples is maintained constant during testing. **Fig. 4** shows a schematic diagram of the used direct shear box apparatus. A circular sample with 2 cm in height and 6 cm in diameter was adopted for testing. Both static and cyclic tests were carried out. In order to evaluate the effect of OCR on the shear strength of the black volcanic ash soil, over-consolidated and normally consolidated samples were tested. For the static testing group, 10 and 50 kPa vertical stresses were adopted for the OC samples, where the OCR is larger than 1. On the other hand, for the Normally-Consolidated (NC) samples, 200 kPa vertical stress was applied with an OCR value equals to 1. Prior to shearing, specimens were consolidated under the designated vertical stress for 1 hour. Then, samples were sheared under undrained condition (constant water content) up to 7 mm at a shearing rate of 0.2 mm/min according to the Japanese Geotechnical Society standards (JGS 0560, 2009).

The cyclic tests were carried out to evaluate the shear strength behavior subjected to earthquake loading. 50 kPa

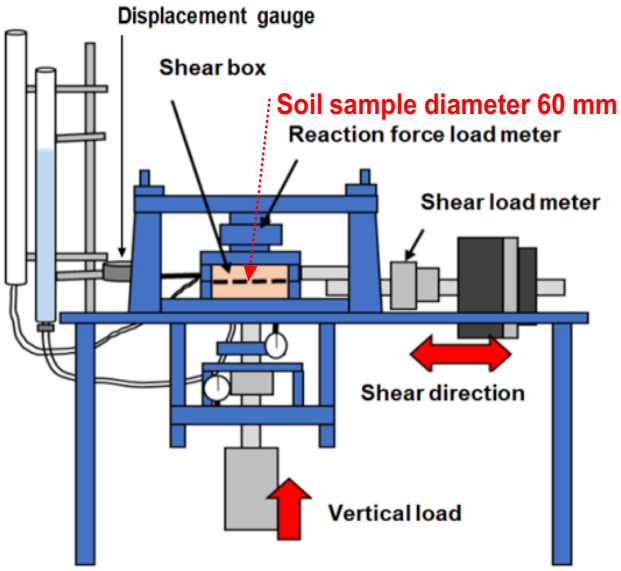

Fig. 4. Schematic diagram of direct shear box test

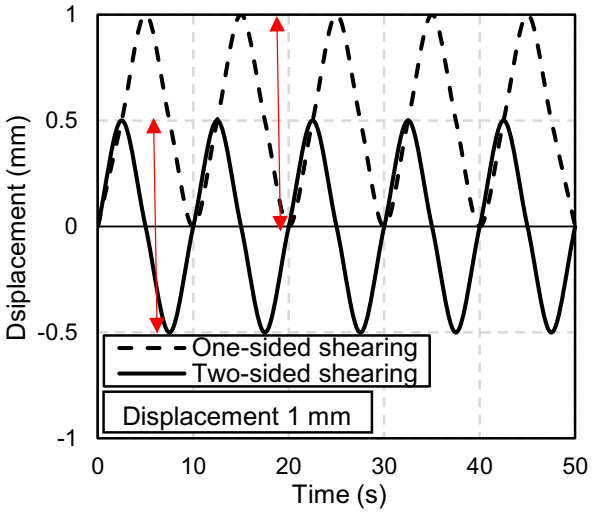

Fig. 5. Cyclic loading patterns (one-sided and two-sided)

vertical stress was applied for the OC samples. While 200 kPa vertical stress for the NC samples was used. Two shearing patterns with a shearing displacement of 1 mm were adopted. The first pattern is one-sided cyclic shearing, while two-sided cyclic shearing corresponds to the second pattern. A schematic diagram illustrating the adopted shearing patterns is shown in **Fig. 5**. For the one-sided cyclic shearing pattern, 1 mm positive displacement was used. While, for the two-sided cyclic pattern, 0.5 mm positive displacement followed by 0.5 mm negative displacement was adopted. For both patterns, the cumulative displacement for each cycle is 2 mm. A total number of 10 cycles was adopted for each pattern. **Table 2** illustrates the testing program and conditions.

2.3.3 Pore size distribution analysis

Soil mass is a collection of soil particles of various sizes and shapes with pores filled with air and water. The Pore-Size Distribution (PSD) is critical in understanding the physical, mechanical, and hydrological behavior of soil (Simms et al., 2001; Saranya et al., 2016; and Niu et al., 2019). Mercury Intrusion Porosimetry (MIP) is a commonly used technique for evaluating the pore size distribution (PSD) for porous media, such as soil and rock. In this technique, mercury at an increasing pressurizing steps is injected into the porous material with the volume of the injected mercury being recorded. (Wang et al., 2016) has developed a simple technique to determine the PSD based on the SWCC. It was reported that the results obtained using this simple technique compare well to the results obtained using the conventional MIP with an excellent correlation. However, the determination of the PSD using the SWCC based technique may be only valid for the drying phase.

Based on that, in this paper, the PSD for the black volcanic ash soil was evaluated based on SWCC corresponding to the drying phase. Adopting this technique, different suction pressures correspond to the penetration of air in pores with different sizes, which can be determined using the Washburn equation (Nimmo, 2014) as follows:

$$d = \frac{4T_S \cos \alpha}{P} \quad [2]$$

where *d* is the soil pore diameter; *Ts* is the surface tension; *α* is the contact angle between the soil particles and the fluid, and *P* is the applied pressure or the capillary/suction pressure.

Table 2. Testing program for static and cyclic loading

Test ID	Sample Condition	Sr_0 (%)	Void ratio (e_0)	Vertical stress (kN/m^2)
Static test				
S01	Unsat-Undisturbed	65.5	4.70	10
S02	Unsat-Undisturbed	68.0	5.16	50
S03	Unsat-Undisturbed	72.5	4.95	200
S04	Sat-Undisturbed	99.7	4.60	10
S05	Sat-Undisturbed	99.3	4.77	50
S06	Sat-Undisturbed	100	4.72	200
SD01	Sat-Disturbed	100	5.10	10
SD02	Sat-Disturbed	100	4.82	50
SD03	Sat-Disturbed	100	5.12	200
One-sided cyclic				
C101	Unsat-Undisturbed	67.8	4.03	50
C102	Unsat-Undisturbed	69.5	4.01	200
C103	Sat-Undisturbed	99.5	4.41	50
C104	Sat-Undisturbed	96.8	4.45	200
CD101	Unsat-Disturbed	80.7	4.82	50
CD102	Unsat-Disturbed	79.4	4.61	200
CD103	Sat-Disturbed	100	4.96	50
CD104	Sat-Disturbed	100	4.90	200
Two-sided cyclic				
C201	Unsat-Undisturbed	74.1	4.73	50
C202	Unsat-Undisturbed	82.9	4.96	200
C203	Sat-Undisturbed	100	4.43	50
C204	Sat-Undisturbed	100	4.77	200
CD201	Unsat-Disturbed	81.6	4.54	50
CD202	Unsat-Disturbed	82.2	4.64	200
CD203	Sat-Disturbed	100	4.49	50
CD204	Sat-Disturbed	100	4.23	200

Note: S: static, C1: cyclic one-sided shearing, C2: cyclic two-sided shearing, Unsat: unsaturated, and Sat: saturated.

3. Results and discussion

3.1 Chemical composition

In order to elaborate the chemical composition of the black volcanic ash soil, XRF analysis was carried out as shown in **Fig. 6**. It was found that the collected black volcanic ash is comprised mainly of SiO_2, Al_2O_3, Fe_2O_3 accounting for as high as about 94%. Those three are the main components forming a substance called allophane. The individual particles of allophane are significantly smaller than other clay minerals and are extremely porous. Allophane is a product of the weathering process of the volcanic ash, where the ash is formed by the rapid cooling of the material generating from volcanic eruptions. The rapid cooling prevents the formation of crystalline structure. For the ash to transform into allophane, it was found that the material from which the ash is originated must be non-crystalline and must remain well-drained during cooling (Wesley, 2002). Several researchers have shown that the allophane molecule is remarkably effective at retaining water (Parfitt, 1990; Rousseaux and Warkentin, 1976).

The ‘rule of thumb’ that ‘allophanic soils always have a high water content’ has been reported by (So, 1995 and Wesley, 2002). Their combined findings using some

allophane soils from New Zealand (NZ) and Indonesia (INA) are illustrated in Fig. 7. In addition, the results corresponding to the black volcanic ash used in this study were added to **Fig. 7** (black circular scatters), where the results fit well following the same trend on the correlation between the allophane content and water content was observed.

Generally, the allophane behavior in response to the external loads (such as compaction and earthquake shakes) is different from that of other clay types. Wesley, 2009 reported that the external load destroys the chemical structure of the allophane, consequently transforming the mineral into an amorphous mass with relatively low strength. In addition, the breakdown of the chemical structure releases large amounts of adsorbed water that is held within that structure, causing a total shear strength reduction of the soil.

3.2 Pore size distribution characteristic

The SWCC corresponding to the undisturbed and disturbed samples of the same black volcanic ash soil was reported by (Alowaisy et al., 2020) as illustrated in **Fig.8**. The newly developed Continuous Pressurization Method (CPM) was adopted to determine the SWCC. The CPM utilizes the axis-translation technique, where a saturated high Air Entry Value (AEV) interface is used to retain the air pressure while allowing the pore water pressure to dissipate by draining the water out of the sample. It can be observed that the SWCC of the undisturbed sample significantly differs from that of the disturbed sample. Furthermore, the disturbed sample has a relatively larger AEV in comparison to the disturbed sample.

Fig. 9 illustrates the PSD of the black volcanic ash soil. Even though both samples have the same bulk density, a significant difference between the undisturbed and disturbed samples was observed, where the cumulative pore volume corresponding to the undisturbed samples was found to be larger than that of the disturbed sample. The undisturbed sample exhibit a dominant pore diameter (one peak) of with an average diameter of 72.8 μm. While for the disturbed sample, two dominant pore diameters (two peaks) were obtained with diameters of 41.6 and 4.9 μm respectively. The difference can be attributed to the pore structure disturbance, where the undisturbed sample exhibits a unimodal pore structure, while the disturbed sample shows a bimodal pore structure. It must be noted that the unimodal distribution indicates the existence of inter pore water only. While a bimodal distribution reflects both an inter pore and intra pore morphology. The inter pore represents the water molecules being bounded between soil aggregates, whereas the intra pore represents the water molecules being bounded within the

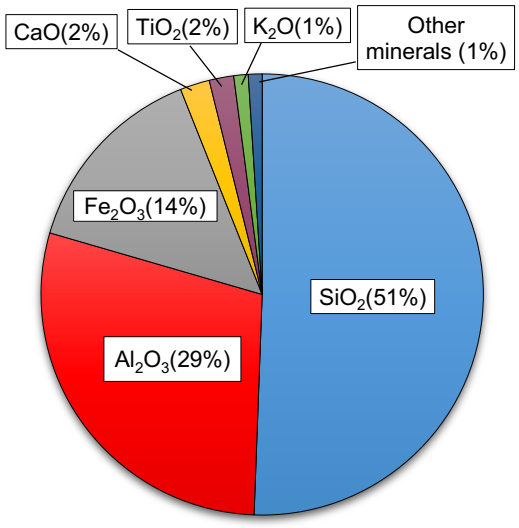

Fig. 6. The chemical composition of the black volcanic ash soil is comprised mainly of SiO_2, Al_2O_3, Fe_2O_3 accounting for as high as about 94%.

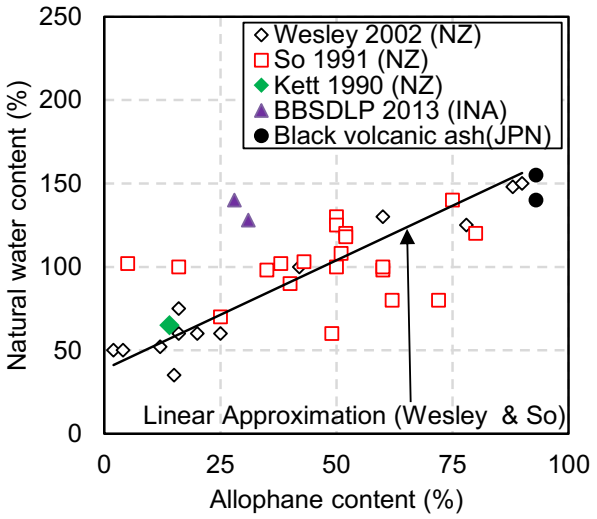

Fig. 7. Natural water content of allophanic soil compared to their allophane content

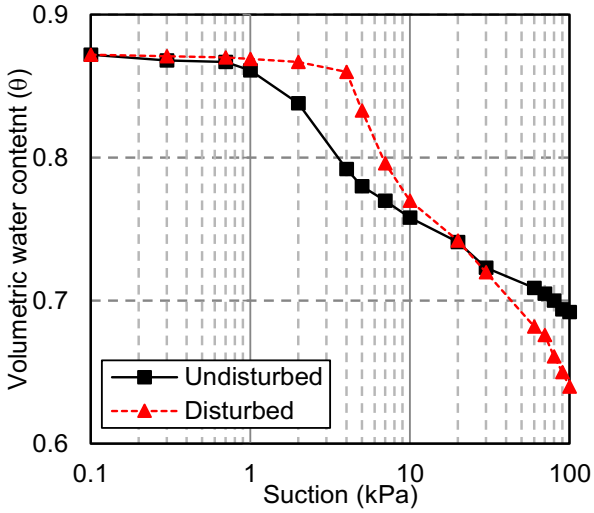

Fig. 8. The soil-water characteristic curve (SWCC) of the black volcanic ash soil

soil aggregates and on the clay particles' surface. Consequently, it can be concluded that the pore structure of the disturbed sample is relatively unstable in comparison to the undisturbed sample.

3.3 Static shearing behavior

The relationship between the shear displacement and the shear stress is shown in **Fig. 10**. Under undisturbed unsaturated conditions, for the NC sample, the shear stress converges to a constant value at a shear displacement of 1.5 mm. While, for the OC sample, the shear stress dramatically increases and converges to a constant value at a shear displacement of about 0.5 mm.

The relationship between the vertical stress and the shear stress for the undisturbed and disturbed samples is illustrated in **Fig. 11**. It can be observed that for the NC condition, the vertical stress increases dramatically till reaching the peak shear stress, followed by a slight decrease regardless of the saturation condition. On the other hand, for the OC condition both vertical stress and shear stress increase without reaching a distinct peak value. The observed behavior is similar to clayey soil behavior under undrained triaxial testing conditions (Atkinson et al., 1987). For the OC condition, the monotonical increase in the vertical stress can be justified to be a result of the pore water pressure reduction during shearing. On the other hand, for the NC condition, the increase of the pore water pressure during shearing induces a reduction in the vertical stress.

For the undisturbed sample, the apparent cohesion decreases from 24.6 kN/m^2 under the unsaturated condition to 13 kN/m^2 for saturated conditions. In addition, the apparent friction angle slightly reduced from 35.5° under the unsaturated condition to 35.1° for the saturated condition. Furthermore, the apparent cohesion decreases dramatically more than 50 % for the saturated disturbed sample condition, while the apparent friction angle slightly degraded to 34.08° in comparison to the undisturbed conditions. This behavior can be related to the effect of soil structure disturbance in the black volcanic ash soil which was elaborated in the PSD characteristics. Finally, it can be concluded that the shear strength strongly depends on the soil structure and water content which is translated into suction forces that contribute significantly to the total shear strength of the soil.

An empirical relationship of the over-consolidated ratio and the shear stress ratio was developed by (Mayne, 1984). The black volcanic ash soil was plotted as shown in **Fig. 12**. The line represents the empirical model, while the scatter plots correspond to the experimental data. For an OCR = 1 the shear stress ratio was found to be 0.55,

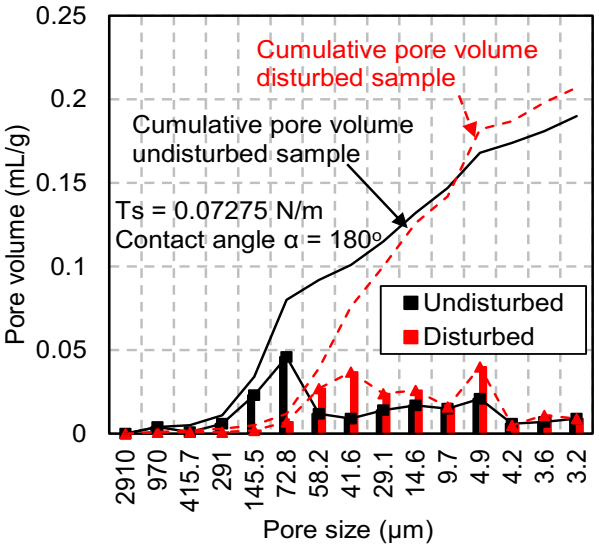

Fig. 9. The pore size distribution of the black volcanic ash soil

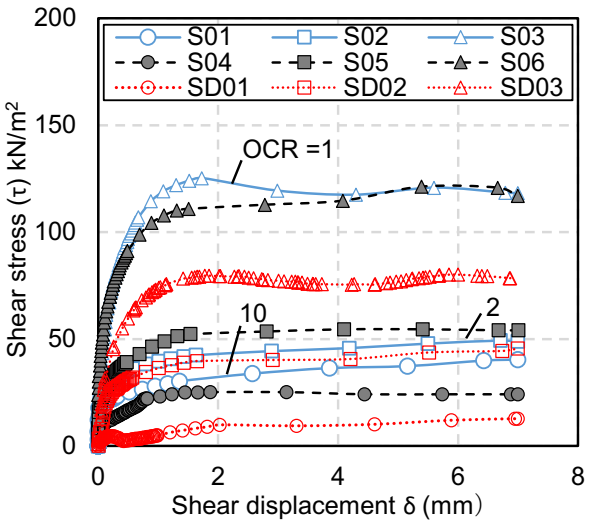

Fig. 10. Relationship of shear stress and shear displacement

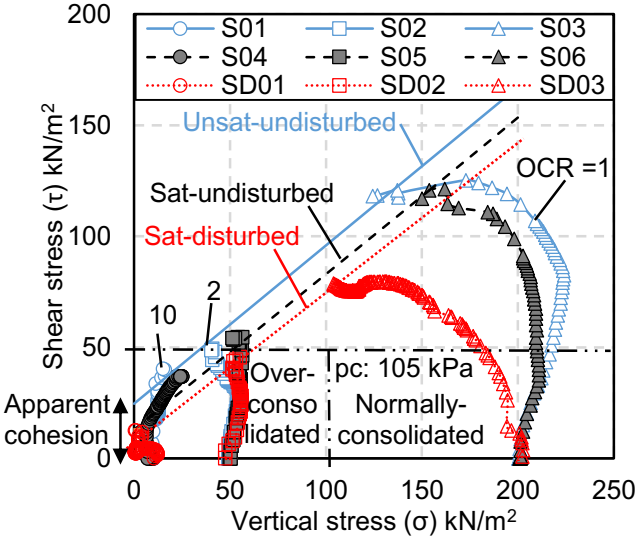

Fig. 11. Stress path for static test of undisturbed and disturbed samples of black volcanic ash soil

where the shear stress ratio increases as the value of the OCR increases.

3.4 Cyclic shearing behavior (one-sided and two-sided)

For the cyclic strain-controlled mode, the normalized vertical stress degradation with the number of cycles (N) can be quantified using the degradation index (δ). Where S_1 and S_N are the initial normalized vertical stress and the normalized vertical stress after N cycles at a constant shear strain amplitude.

$$\delta = \left(1-\frac{\sigma_{SN}/\sigma_0}{\sigma_{S1}/\sigma_0}\right) = \left(1-\frac{\sigma_{SN}}{\sigma_{S1}}\right) \quad [3]$$

In general, for the one-sided cyclic shearing, the normalized vertical stress decreases by increasing the number of cycles. Consequently, the reduction in the normalized vertical stress leads to a reduction in the total shear strength of the soil (Matsuda et al., 2011). The reduction of the normalized vertical stress might be associated with an increase of the pore water pressure during the shearing test.

The relationship between the degradation index of the cyclic normalized vertical stress and the number of cycles for the OC and NC samples are illustrated **in Fig. 13** and **Fig. 14** respectively. A significant difference between the undisturbed and disturbed samples can be observed. The degradation index value corresponding to the disturbed sample is 20 % higher than that of the undisturbed sample, where for both conditions the degradation index increases by increasing the number cycles. In other words, the cyclic normalized vertical stress of disturbed samples degrades faster than that of the undisturbed samples under cyclic loading. It must be noted that for both OC and NC samples, the normalized vertical stress shows a similar reduction tendency. The normalized vertical stress decreases immediately at the beginning of the shearing. It can be concluded that the effect of the soil structure disturbance can be observed in the cyclic normalized vertical stress degradation, where the degradation index of the cyclic normalized vertical stress is higher for the disturbed samples which can be attributed to the unstable micro-pore structure.

On the other hand, the degradation index of the cyclic normalized vertical stress in the NC samples was found to be larger than that of the OC samples. This trend can be attributed to the increase in the pore water pressure during shearing. The generated pore water pressure is significantly lower for OC samples in comparison to the NC samples.

Furthermore, the degradation index tends to be lower for the unsaturated conditions than that of the saturated conditions for both OC and NC samples.

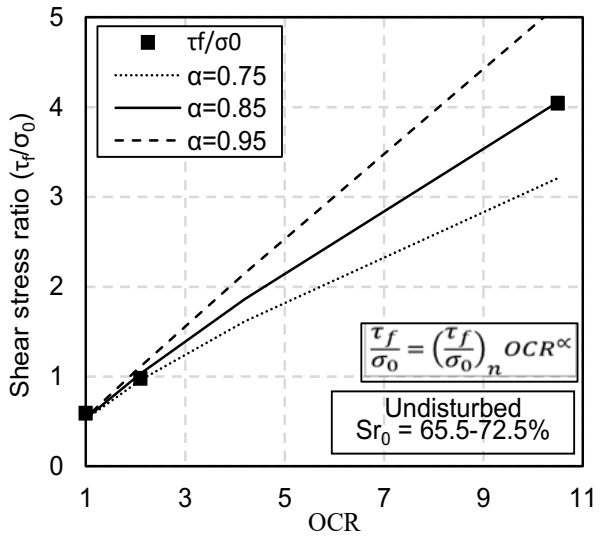

Fig. 12. Relationship of normalized shear stress at the end of shearing and over-consolidation ratio

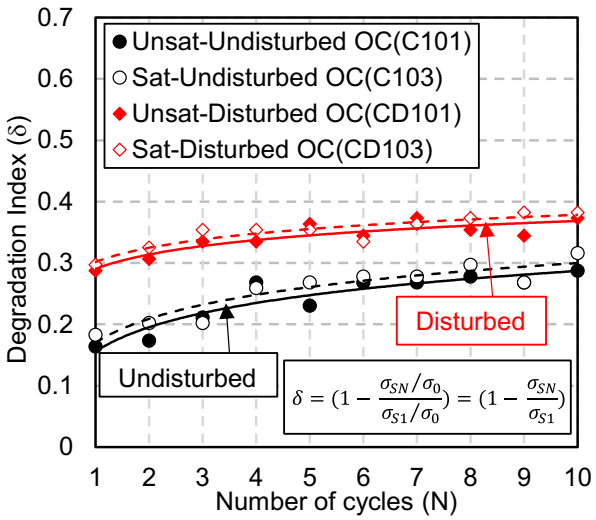

Fig. 13. Degradation index (δ) of OC undisturbed and disturbed samples.

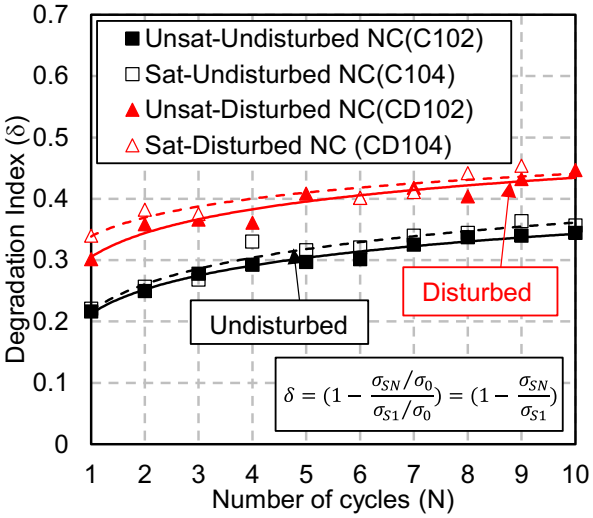

Fig. 14. Degradation index (δ) of NC undisturbed and disturbed samples.

It can be said that the total shear strength of the soil strongly depends on the water content, which can be translated into suction forces which contribute to the total shear strength.

The relationship between the normalized shear stress and the number of cycles for the NC samples under one-sided and two-sided shearing patterns are shown in **Fig. 15** and **Fig. 16** respectively. The normalized shear stress corresponding to the undisturbed samples is 10% higher than that of the disturbed samples. On the other hand, a significant difference in the shear stress development pattern was observed. For the one-sided cyclic shearing, the test results showed that the normalized shear stress reduces starting from the first cycle for both disturbed and undisturbed samples. While significantly higher normalized shear stress value was obtained under the two-sided cyclic shearing test in comparison to the one-sided cyclic shearing test. It can be seen that the increasing number of cycles leads to a monotonical increase in the normalized shear stress value till reaching the maximum value after 10 cycles (last cycle). This can be attributed to the increase in the frictional resistance of the soil due to the shear displacement direction. The results also compare well to two-sided cyclic shearing direct shear box test results reported by (Putra et al., 2019). It was reported that increasing the number of cycles results in increasing the normalized shear stress for the strain-controlled test. Finally, it can be concluded that the cyclic shearing pattern and direction significantly influence the total shear strength of the soil.

Also, it can be recognized that the normalized shear stress of unsaturated conditions is slightly larger than that of the saturated conditions. It can be related to the suction forces' contribution to the total strength of the soil, where the interparticle forces due to the suction in the unsaturated condition is higher than that of saturated condition.

3.5 Correlation of the average degradation index and the peak static shear stress ratio

In order to evaluate the correlation of the degradation index and the static shear stress ratio, the degradation index (δ_{avg}) from the first cycle till the final cycles is plotted against the peak static shear stress ratio (τ_p/σ_0) for the whole soil samples as illustrated in **Fig. 17**. It can be observed that low static shear stress ratio (τ_p/σ_0) imposes relatively higher average degradation index. It can be concluded that the normalized vertical stress reduction during the cyclic loading strongly depends on the average degradation index.

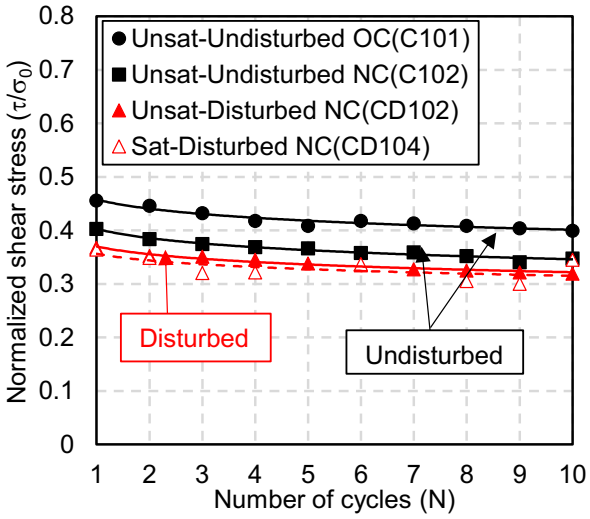

Fig. 15. Normalized shear stress ratio for one-sided shearing pattern corresponding to undisturbed and disturbed samples

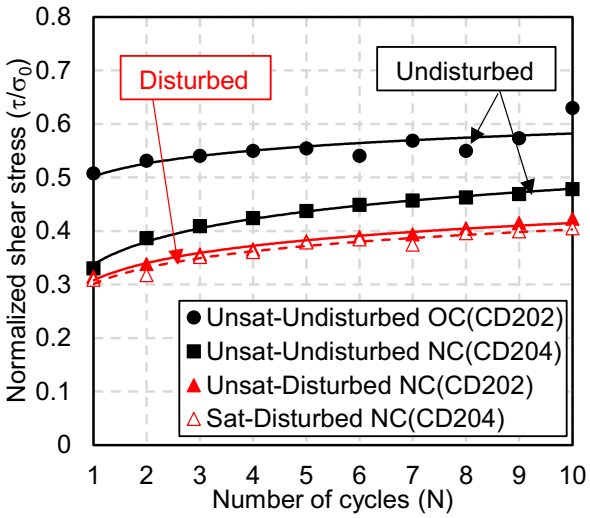

Fig. 16. Normalized shear stress ratio for two-sided shearing pattern corresponding to undisturbed and disturbed samples

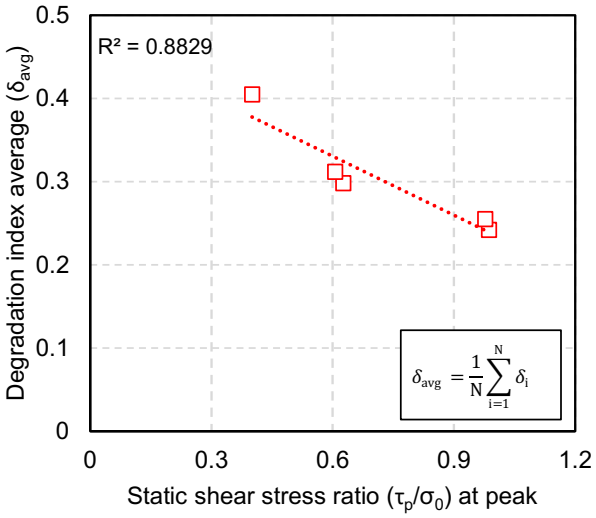

Fig. 17. Relationship between average degradation index and peak static shear stress ratio

Conclusions

Through this paper, the chemical composition of the black volcanic ash soil was evaluated using the X-ray fluorescence analysis. In addition, the pore size distribution reflected from the soil-water characteristic curve (SWCC) has been evaluated. The shear strength characteristic of the black volcanic ash soil was investigated using a constant volume direct shear box apparatus under static and cyclic loading.

It was found that the chemical composition of black volcanic ash soil is comprised mainly from SiO_2, Al_2O_3, Fe_2O_3 which accounts for as high as about 94%. It is known that these three are the main components forming a substance called allophane. The undisturbed samples exhibit a unimodal pore structure and the disturbed samples exhibit a bimodal pore structure. Since the pore structure of the disturbed sample is unstable, the static shear strength tends to be lower, and the degradation index value is 20% higher than that of the undisturbed sample. In other words, the cyclic normalized vertical stress of disturbed samples degrades faster under cyclic loading.

The degradation index value in the normally consolidated samples was found to be larger than that of the over-consolidated samples. It might be associated with the increase in the pore water pressure during shearing, where the pore water pressure reduction in the over-consolidated samples is lower than that of the normally consolidated samples. In addition, the normalized vertical stress and the shear stress of the unsaturated samples under static and cyclic loading is larger than that of saturated samples. This can be related to the influence of the suction forces which contribute to the total shear strength of the soil.

Finally, a good correlation between the average degradation index (δ_{avg}) and the static shear stress ratio (τ_p/σ_0) was obtained. A lower static shear stress ratio (τ_p/σ_0) imposes a higher average degradation index.

Acknowledgement

The authors express their gratitude to the laboratory technical assistant Mr. Michio Nakashima for their great support.

References

Albrook, R. F., 1985. The effect of allophane on soil properties. Applied Clay Science, **1**: 65-69

Alowaisy, A., Yasufuku, N., Ishikura, R., Hatakeyama, M., Kyono, S., 2020. Continuous pressurization method for a rapid determination of the soil water characteristics curve for remolded and undisturbed cohesionless soils. Soils and Foundations, **66** (3): 634-647

Atkinson, J. H., Richardson, D., 1987. The effect of local drainage in shear zones on the undrained strength of overconsolidated clay. Geotechnique, **37** (3): 393-403

Chiaro, G., Umar, M., Kiyota, T., Massey, C., 2018. The Takanodai landslide, Kumamoto, Japan: insights from post-earthquake field observations, laboratory tests, and numerical analyses. Proc. Geotechnical Earthquake Engineering and Soil Dynamics V, June 10-13, 2018, Austin, Texas: 98-111

Ding, Z., Kong, B., Wei, X., Zhang, M., Xu, B., Zhao, F., 2019. Laboratory testing to research the microstructure and dynamic characteristics of frozen-thawed marine soft soil. Journal of Marine Science and Engineering, **7** (85): 1-19

Japan Soil Inventory., 2016. National Agriculture Industry Research Organization

Kitazono, Y., Suzuki, A., Kajiwara, M., Aramaki, S., 1987. Contribution of microstructure to repeated loading effect on compacted allophaneous volcanic ash soil. Soils and Foundations, **27** (4): 23-33

Kiyota, T., Ikeda, T., Konagai, K., Shiga, M., 2017. Geotechnical damaged caused by the 2016 Kumamoto earthquake, Japan. International of Journal Geoengineering Case Histories, **4** (2): 78-95

Kodani, Y., Kuono, S., Uchida, K., 1975. Relation between Organic Matter, Content and Physical Properties of Kuroboku Soil. The Japanese Society of Irrigation, Drainage and Reclamation Engineering, **60**: 7-13

Matsuda, H., Hendrawan, A. P., Ishikura, R., Kawahara, S., 2011. Effective stress change and post-earthquake settlement properties of granular materials subjected to multi-directional cyclic simple shear. Soils and Foundations, **51** (5): 873-884

Mayne, P. W., 1984. K_0−C_u/σ_{u0} Trends for Overconsolidated Clays. Journal of Geotechnical Engineering, **110** (10): 1511

Miyabuchi, Y., 2016. Landslide disaster triggered by the 2016 earthquake in and around Minamiaso village, western part of Aso caldera, southwestern Japan. Journal of Geography, **125** (3): 421-429

Mshana, N.S., Suzuki, A., Kitazono, Y., 1993. Effect of weathering on stability of natural slopes in north-central Kumamoto. Soils and Foundations, **33** (4): 74-87

Mukonoki, T., Kasama, K., Murakami, S., Ikemi, H., Ishikura, R., Fujikawa, T., Yasufuku, N., Kitazono, Y., 2016. Reconnaissance report on geotechnical damage caused by an earthquake with JMA seismic intensity 7 twice in 28 h, Kumamoto, Japan. Soils and Foundations, **56** (6): 947-964

Nimmo, J. R., 2004. Porosity and Pore Size Distribution. Elsevier, **3**: 295-303

Niu, G., Sun, D., Shao, L., Zeng, L., 2019. The water retention behaviours and pore size distributions of undisturbed and remoulded complete-intense weathering mudstone. European Journal of Environmental and Civil Engineering, 1-17

Parfitt, R., 1990. Allophane in New Zealand. Australian Journal of Soil Research, (28): 343-360

Putra, O. A., Yasufuku, N., Ishikura, R., Alowaisy, A., Kawaguchi, Y., 2019. Mechanical behaviour of unsaturated undisturbed black volcanic ash soil under static and cyclic loading. Proc. 7th International Symposium on Deformation Characteristics of

Geomaterials (IS-Glasgow 2019), June 26-28, 2019, Glasgow: 92

Qinghui, L., Jiajia, Y., Jian, Z., Zhigang, C., 2016. Microstructure study on intact clay behavior subjected to cyclic principal stress rotation. Proc. International Conference on Transportation Geotechnics, September 4-7, 2016, Portugal: 991-998

Rousseaux, J., and Warkentin, B., 1976. Surface properties and forces holding water in allophane soils. Soil Science of America Journal, **40** (3): 446-451

Saranya, N., and Arnepalli, D. N., 2016. Effect of pore size distribution on unconfined compressive shear strength. Proc. Indian Geotechnical Conferences, December 15-17, 2016, India

Simms, P. H., and Yanful, E. K., 2001. Measurement and estimation of pore shrinkage and pore distribution in a clayey till during soil water characteristic curve tests. Canadian Geotechnical Journal, **38**: 741-754

So, E., 1995. Influence of allophane content on the reactivity and pore size distribution of lime stabilized volcanic soil. Journal of the Society of Materials Science Japan, **44** (503), 1007-1010.

Wang, M., Pande, G. N., Kong, L. W., Feng, Y. T., 2016. Comparison of pore-size distribution of soils obtained by different methods. International Journal of Geomechanics, Technical Note 06016012

Wesley, L., 2002. Geotechnical properties of two volcanic soils. University of Auckland.

Wesley, L., 2009. Behaviour and geotechnical properties of residual soils and allophane clays. Obras y Proyectos, (6): 5-10

Yamauchi, Y., 1983. Kyushu University Press, in Japanese

Symbols and abbreviations

d	Soil pore diameter
MIP	Mercury Intrusion Porosimetry
N	Number of cycles
NC	Normally consolidated
OC	Over-consolidated
OCR	Over-Consolidated Ratio
P	Applied pressure
PSD	Pore-size distribution
Pc	Yield stress
$P_{o'}$	Overburden pressure.
SEM	Scanning Electron Microscope
SWCC	Soil-water characteristic curve
S_1	Initial normalized vertical stress
S_N	Normalized vertical stress after N cycles
Ts	Surface tension
XRF	X-ray fluorescence analysis
α	Contact angle between the soil particles and the fluid
τ	Shear stress
σ	Vertical stress
δ	Degradation index
δ_{avg}	Average degradation index
τ_p	Peak static shear stress ratio